HHS Public Access

Author manuscript

Conf Proc IEEE Eng Med Biol Soc. Author manuscript; available in PMC 2019 April 15.

Published in final edited form as:

Conf Proc IEEE Eng Med Biol Soc. 2018 July ; 2018: 1380–1383. doi:10.1109/EMBC.2018.8512503.

Graph-Based Models of Cortical Axons for the Prediction of Neuronal Response to Extracellular Electrical Stimulation

Clayton S. Bingham [Student Member, IEEE], **Jean-Marie C. Bouteiller [Member, IEEE]**, **Dong Song [Member, IEEE]**, and **Theodore W. Berger [Fellow, IEEE]**

University of Southern California, CA, USA

Abstract

Over the past decade, many important insights to brain function have been obtained through clever application of detailed compartmental model neurons. New computing capabilities brought opportunities to study large networks of model neurons. Certain applications for these models, such as extracellular electrical stimulation, demand a very high degree of biological realism. While dendrites and somatic morphology may be obtained from explicit reconstructions, this approach is less useful for axonal structures, which are more difficult to characterize across a neuronal population. The purpose of this paper is to extend neuronal morphology generative models to highly branched axon terminal arbors as well as to present a clear use-case for such models in the study of cortical tissue response to externally applied electric fields. The results of this work are (i)presentation and quantitative/qualitative description of generated fibers and (ii) an extracellular electrical stimulation strength-duration study.

I. Introduction

The unique, but well described, geometry of the hippocampus is a strong determinant of spatial and temporal patterns of activity. To reliably reproduce these activation patterns many computational studies require the use of morphologically detailed implementations of neurons, including axons. This need is particularly evident when modeling tissue response to extracellular stimulation, where explicit morphologies aid the prediction of activation thresholds under various conditions [1–3]. Prominent methods involve deliberate arrangement of biologically realistic neuronal structures in virtual space to reconstruct elements of the tissue system being studied [4,5]. This critical step ensures fiber excitability is appropriately modulated due to location and orientation within electromagnetic fields. However most of the biological realism in these studies is reserved for dendritic arbors rather than axonal. This disparity becomes especially conspicuous when modeling highly branched fibers of cortical tissue rather than relatively straight and long peripheral nerves. Deliberate arrangement of neuronal structures is also important for accurate prediction of endogenous electric fields and tissue-tissue interactions, including: (i) local field potentials (LFPs) and (ii) the region- specific impact of ephaptic coupling, etc. Having explicitly modeled neuronal structures enforces the realism of conduction delays between connected

correspondence csbingha@usc.edu.

populations of neurons. This realism may be necessary to study emergent network activity such as co-oscillatory activity in hippocampal networks [6,7].

Minimum spanning trees, constructed via greedy algorithms, are an efficient approach to reconstructing trees using points extracted from images [8,9]. By using images, a great deal of biological realism is forced onto the resulting graph, validating the approach. However, when growing a minimum spanning tree from points sampled at random from a volmne representing a terminal field, the result is less than biological, owing to the extreme path lengths that often result. One demonstrated approach to moderating this outcome is to balance the minimization of membrane against path length [10–13]. However, optimizing this balance is intractable because these objective functions are in direct conflict causing solutions to be inefficient, inaccurate, or both [14–18]. Another unaddressed challenge to using this general approach is the maintaining of appropriate morphometries, such as bifurcation angle, branch extension angle, etc. Use of a balancing factor can indirectly assert a modicum of control over these but prominent models do not allow explicit morphometric thresholds to be set. This represents a significant limitation of these prior efforts: arbor features such as bifurcation angles, branch extension angles, and inter-bifurcation length have a clear impact on brandling patterns and, therefore, spatiotemporal patterns of activity.

This paper presents a new graph-based algorithm that rectifies these limitations. To demonstrate the utility of this model for examination of cortical stimulation, this paper also presents a study of the impact of arbor topography and morphometry on activation thresholds and, by extension, spatiotemporal patterns of activity in the hippocampus. The results of this work comprise (i) a description of the generative algorithm proposed, (ii) presentation and qualitative description of generated fibers, and (iii) an extracellular electrical stimulation strength-duration study.

II. Methods

While it may one day become important to recalibrate models for more exacting morphometrics gathered by experimentalists, the approach presented in this paper focuses on accurately capturing the emergent spatial features of spiny stellate entorhinal cortical axons in sprague dawley rats, where it is important that (i) fibers are constrained within the septotemporal axis to approximately 1-1.5mm, (ii) laminar organization along the transverse axis is inviolate, with medial and lateral entorhinal cortical axons confined to the middle and outer thirds of the dentate molecular layer, respectively , and (iii) axons synapse with a pronounced *en passant* connective schema, where most pre-synaptic boutons are non-terminal [19–21]. The method whereby this is accomplished is best described as greedy and graph-based: nodes and edges are connected to minimize wiring costs while satisfying criteria comprising spatial and morphometric constraints.

A. Determination of Carrier-Points

Many emergent features of spatial graph/tree generative models are determined by the number and spatial distribution of nodes or carrier-points, therefore the selection of carrier points is a critical step in successful generation of biologically appropriate axonal trees. Previous work has been done to elucidate the number and distribution of the points which

form the bulk of carrier-points for entorhinal cortical axons within the dentate perforant path [22–24]. In short, the number of spines in the outer and middle third of hippocampal granule cell dendritic arbors, the number/density of granule cells, and the number/density of entorhinal cortical cells contributing to the perforant path provides the arithmetic for deducing the number of synapses made in each axon terminal field. Coupled with data on the septal-temporal domain of these axons, carrier-points can be distributed throughout the volume of a plausible hypothetical terminal field.

B. Growing an Axon from Carrier-Points

While much of the challenge of generating functional axons lies with the selection of suitable carrier-points, encouraging biological realism requires additional non-trivial steps to constrain branching features of generated topologies. Fig. 2 diagrams the proper preprocessing and successful execution of the algorithm used to generate the trees used in the analyses presented in later sections of this manuscript.

Following development and testing of this algorithm, a function was added to automatically export generated neural simulation environments. Later in this paper, extracellular electrical stimulation studies performed with the generated morphologies are presented to demonstrate the maturity of this pipeline.

C. Strength-Duration Relationship in Response to Extracellular Electrical Stimuli

To understand how fiber geometry in the hippocampus gives rise to patterns of activity, fibers were simulated in response to a range of extracellular current source-arbor distances and stimulus amplitudes. Monopole point-source anodal stimuli were used in all of the stimulation experiments presented in this article. Tonic (step-function) current was applied extracellularly, 250μm from the nearest neuronal compartment. Stimulation was delivered over a range of current amplitudes (current controlled stimulation from an ideal source) designed to cover, at a minimum, rheobase to twice rheobase in 50 equal increments.

Volmne resistivity was set based on 1kHz pulse-frequency, according to experimental data [25]. Volmne conductor capacitance was ignored due to the very low frequency (long unitary pulses) of stimulation being studied [26].

Entorhinal cortical axons in the perforant path are very small and unmyelinated with diameters reported by [19] (~0.1um) and [27] (~0.7μm), corresponding to stem and bouton sizes, respectively. Images of spiny stellate fibers from [19] show the continuous fibers with ‘periodic varicosities’, or non-terminal synaptic boutons on the *en passant* fibers. A series of fibers were generated and instantiated in the simulation enviromnent, NEURON (Yale) [28]. Using Hodgkin-Huxley membrane biophysics under *in vivo* temperature conditions and d-lambda rules to determine appropriate space constants for compartmentalization of the fibers, a strength-duration curve was generated.

III. Results

Results comprise the presentation of fibers grown using the novel algorithm, a strength-duration curve, and an analysis of entorhinal cortical fiber temporal distribution in response to extracellular stimulation at different amplitudes.

The fibers presented in Fig. 3 capture the principle features of entorhinal cortical layer II spiny stellate axons found in the perforant path of the rat dentate gyms. The fibers exhibit (i) distinct laminar organization in the middle and outer thirds of the dendritic region of the dentate, (ii) complete coverage of the entire transverse arc of the dentate, (iii) few terminal branchlets (i.e. *en passant*), and (iv) primary bifurcation at/near the dentate crest.

Fiber activity presented in Fig. 4 yields a plausible pattern of fiber recruitment in response to increasing current densities near the membrane of the fiber sourcing from stimulation applied 250μm away. Due to anodal stimulation, the nearest compartment was always the first site of action potential initiation. The time of AP propagation to any particular compartment in the complex fiber could be shortened by as much as 5ms at 2x rheobase relative to rheobase. 2x rheobase was 139μA. Because time-to-first AP in response to very long pulses is measured along the horizontal axis rather than pulse-width, accurate clironaxie estimation is not reported here.

IV. Discussion

Access to computational power has grown dramatically in the past decade, creating opportunities for neural models of greater complexity. Biologically realistic neural modeling lias outpaced experimental studies in many areas of inquiry. These models provide a testbed for new hypotheses and an established approach to obtaining preliminary data that justify follow-on *in vitro* or *in vivo* studies. One such area of opportunity for this type of modeling is extracellular electrical stimulation and recording. Our incomplete understanding of the interface between devices and neural tissue creates a need for sound approaches to generating functional neuronal models, including their axons, that can be refined as the quantity and quality of experimental data improves. The modeling approach presented in this paper demonstrates this utility.

V. Conclusion

In conclusion, this study represents a step forward for detailed computational modeling of complex neuronal systems. Where previous and noteworthy models were either focused on peripheral axons, where less complex arbors can be considered, or used sophisticated methods to generate dendritic trees but neglected axons altogether, the model presented herein demonstrates an approach to constructing functional axonal morphologies that can be used to study diverse applications, including extracellular electrical stimulation of the cortex.

Acknowledgments

This work was supported by the U.S. National Institutes of Health (Grant 1U01GM104604). Computation was supported by the USC Center for High-Performance Computing and Communications.

References

[1]. Ranck JB (1975). Which elements are excited in electrical stimulation of mammalian central nervous system: A review. Brain Research, 98*(3),* 417–440. [PubMed: 1102064]

[2]. Nowak LG, & Bullier J (1998). Axons, but not cell bodies, are activated by electrical stimulation in cortical gray matter. Experimental Brain Research, 118(A), 477–488. [PubMed: 9504843]

[3]. Nowak LG, & Bullier J (1996). Spread of stimulating current in the cortical grey matter of rat visual cortex studied on a new in vitro slice preparation. Journal of Neuroscience Methods, 67*(2),* 237–248. [PubMed: 8872891]

[4]. Hentall ID, Zorman G, Kansky S, & Fields HL (1984). Relations among threshold, spike height, electrode distance, and conduction velocity in electrical stimulation of certain medullospinal neurons. Journal of Neurophysiology, 51*(5).*

[5]. Joucla S, & Yvert B (2012). Modeling extracellular electrical neural stimulation: From basic understanding to MEA-based applications. Journal of Physiology-Paris, 106(3), 146–158.

[6]. Fries P (2005). A mechanism for cognitive dynamics: neuronal communication through neuronal coherence. Trends in Cognitive Sciences, 9(10), 474–480. http://doi.Org/10.1016/j.tics.2005.08.011 [PubMed: 16150631]

[7]. Whittington MA, Stanford IM, Colling SB, Jefferys JGR, & Traub RD (1997). Spatiotemporal patterns of γ frequency oscillations tetanically induced in the rat hippocampal slice. The Journal of Physiology, 502(3), 591–607. [PubMed: 9279811]

[8]. Prim RC (1957). Shortest Connection Networks And Some Generalizations. Bell System Technical Journal, 36*(6),* 1389–1401.

[9]. Choromanska A, Chang S-F, & Yuste R (2012). Automatic Reconstruction of Neural Morphologies with Multi-Scale Tracking. Frontiers in Neural Circuits, 6, 25 10.3389/fncir.2012.00025 [PubMed: 22754498]

[10]. Cuntz H, Forstner F, Borst A, Hausser M, Kuhlman S, & Saggau P (2010). One Rule to Grow Them All: A General Theory of Neuronal Branching and Its Practical Application. PLoS Computational Biology, 6(8), el000877.

[11]. Cuntz H, Borst A, & Segev I (2007). Optimization principles of dendritic structure. Theoretical Biology and Medical Modelling, 4*(1),* 21 10.1186/1742-4682-4-21 [PubMed: 17559645]

[12]. Cherniak C (1992). Local optimization of neuron arbors. Biological Cybernetics, 66*(6),* 503–510. 10.1007/BF00204115 [PubMed: 1586674]

[13]. Budd J, & Kisvarday Z (2012). Communication and wiring in the cortical connectome. Frontiers in Neuroanatomy, 5(68), 37–49.

[14]. Hu TC (1974). “Optimum Communication Spanning Trees.” SIAM. J of Comput 3, 188–195.

[15]. Alpert CJ, Hu TC, Huang JH, Kahng AB and Karger D, “Prim-Dijkstra tradeoffs for improved performance-driven routing tree design,” in IEEE Transactions on Computer-Aided Design of Integrated Circuits and Systems, vol. 14, no. 7, pp. 890–896, 7 1995.

[16]. Khuller S, Raghavachari B & Young N Balancing minimum spanning trees and shortest-path trees, Algorithmica (1995) 14: 305.

[17]. Wu BY, Chao K-M, Tang CY (2000). Approximation algorithms for some optimum communication spanning tree problems, Discrete Applied Mathematics, Vol. 102:3, pgs. 245–266,

[18]. Gastner MT, Newman MEJ Shape and efficiency in spatial distribution networks. J. Stat. Mech (2006) P01015 https://doi.Org/10.1088/1742-468/2006/01/P01015

[19]. Tamamaki N, Nojyo Y. (1993). Projection of the entorhinal layer II neurons in the rat as revealed by intracellular pressure-injection of neurobiotin. Hippocampus, 3(4), 471–80. [PubMed: 8269038]

[20]. Witter MP (2007). The perforant path: projections from the entorhinal cortex to the dentate gyrus. Prog. Brain Res Vol. 163:43–61. 10.1016/S0079-6123(07)63003-9 [PubMed: 17765711]

[21]. Bindocci E, Savtchouk I, Liaudet N, Becker D, Carriero G, Volterra A (2017). Three-dimensional Ca2+ imaging advances understanding of astrocyte biology. Science. Vol. 356:6339.

[22]. Bingham CS, Loizos K, Yu GJ, Gilbert A, Bouteiller J-MC, Song D, Lazzi G, Berger TW (2018). Model-Based Analysis of Electrode Placement and Pulse Amplitude for Hippocampal Stimulation. IEEE Transactions on Biomedical Engineering, vol. PP, no. 99, pp. 1–1. doi: 10.1109/TBME.2018.2791860

[23]. Bingham CS, Loizos K, Yu GJ, Gilbert A, Bouteiller J-MC, Song D, Lazzi G, Berger TW (2016). A large-scale detailed neuronal model of electrical stimulation of the dentate gyrus and perforant path as a platform for electrode design and optimization .IEEE Engineering in Medicine and Biology Society (EMBC), Orlando, FL, pp. 2794–2797. doi: 10.1109/EMBC.2016.7591310

[24]. Claiborne BJ, Amaral DG and Cowan WM (1990), Quantitative, three-dimensional analysis of granule cell dendrites in the rat dentate gyrus. J. Comp. Neurol, 302: 206–219. [PubMed: 2289972]

[25]. López-Aguado L et al. (2001). Activity-dependent changes of tissue resistivity in the CA1 region in vivo are layer-specific: Modulation of evoked potentials. Neuroscience, 108(2), 249–262. [PubMed: 11734358]

[26]. Gabriel C et al. (1996). The dielectric properties of biological tissues: I. Literature survey. Physics in Medicine and Biology, 41(11), 2231–49. [PubMed: 8938024]

[27]. Naftstad PHJ (1967). An electron microscope study on the termination of the perforant path fibres in the hippocampus and the fascia dentata. Zeitschrift Fur Zellforschung. 76:532–542.

[28]. Hines ML and Camevale NT The NEURON simulation environment In: The Handbook of Brain Theory and Neural Networks, 2nd ed, edited by Arbib MA. Cambridge, MA: MIT Press, 2003, pp. 769–773.

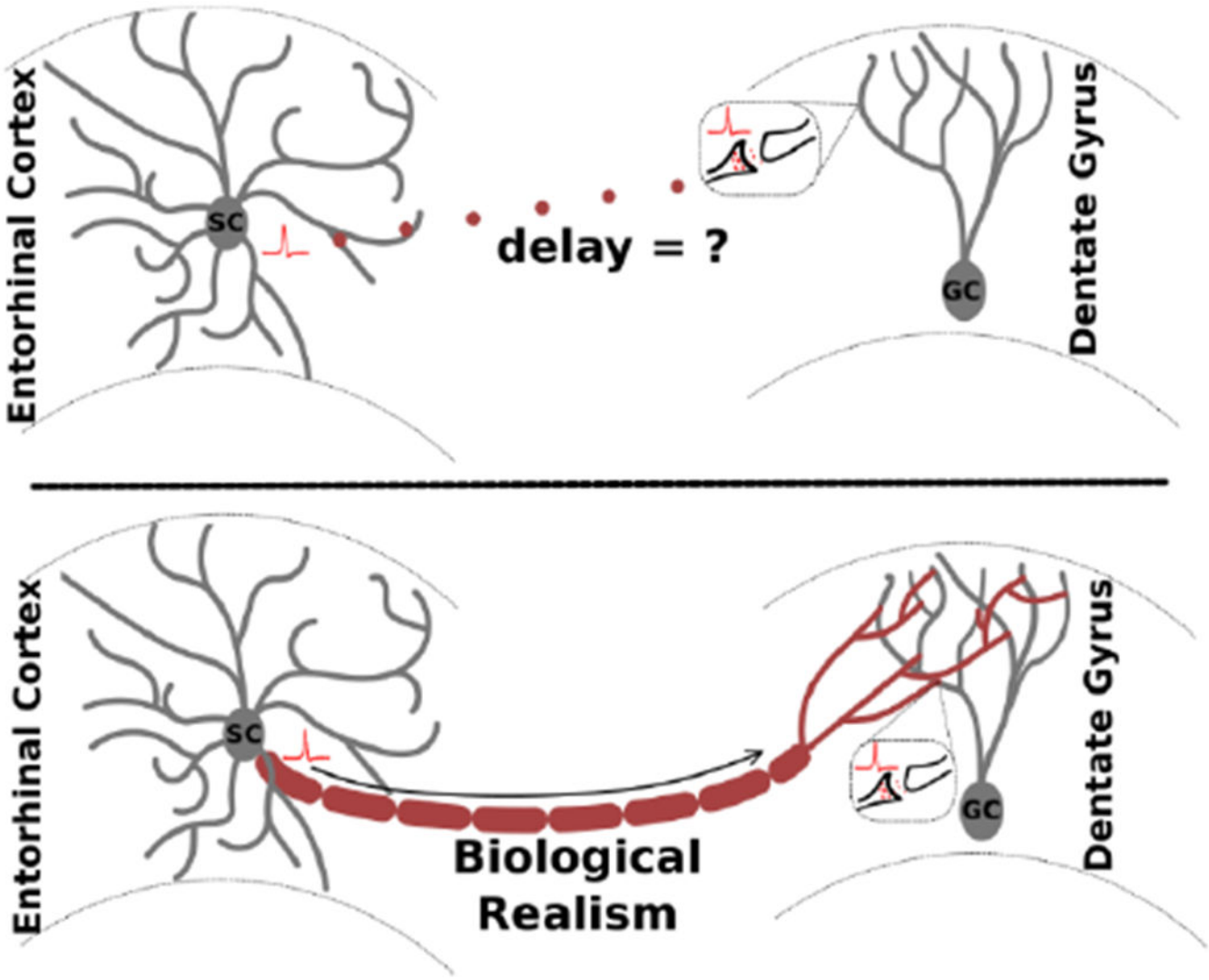

Fig. 1.

Adding biological realism to axon models for the study of extracellular electrical stimulation allows more accurate analysis of neural network activity.

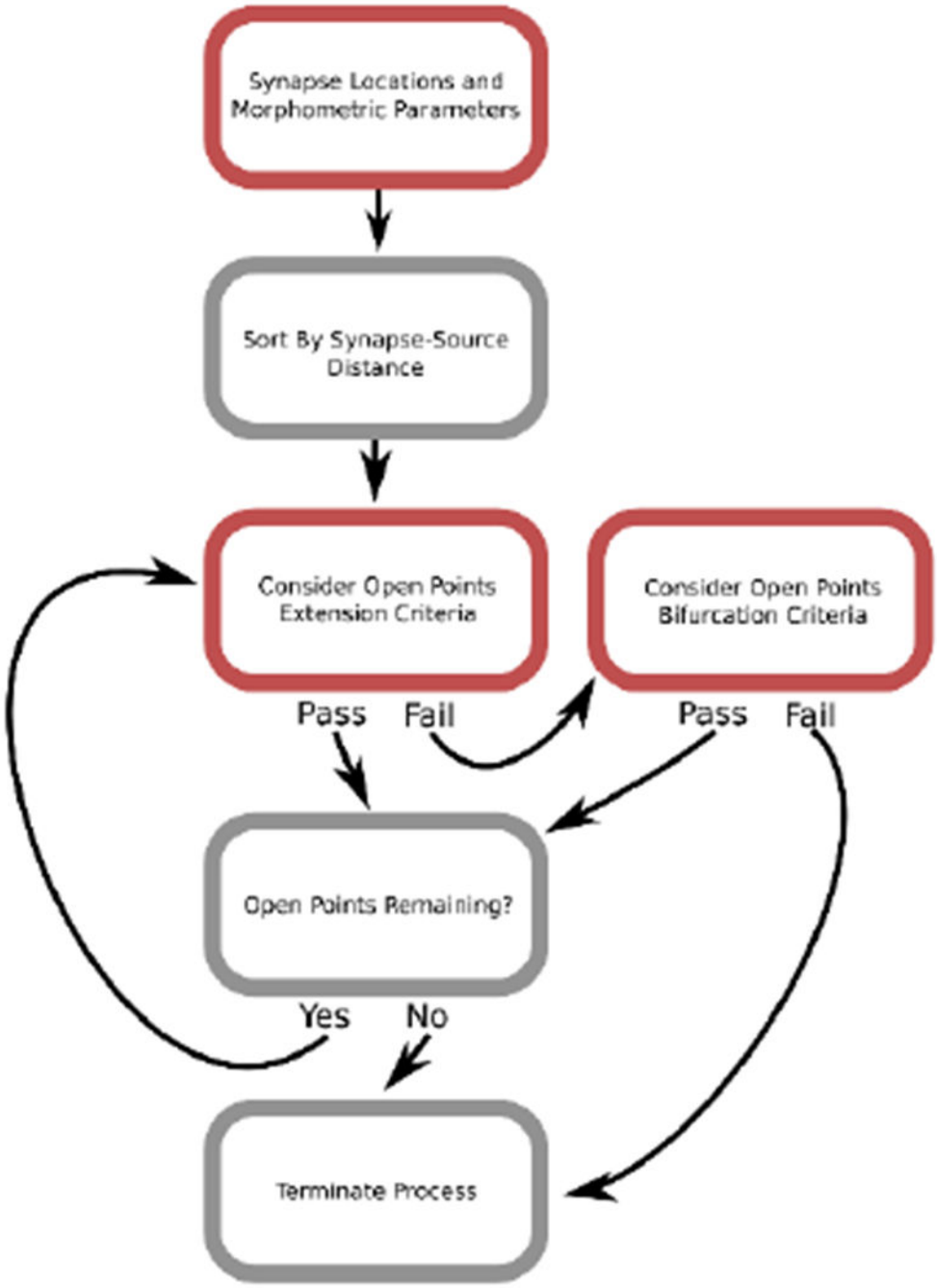

Fig. 2.
The basic approach to growing morphometrically realistic fibers from a set of carrier points.

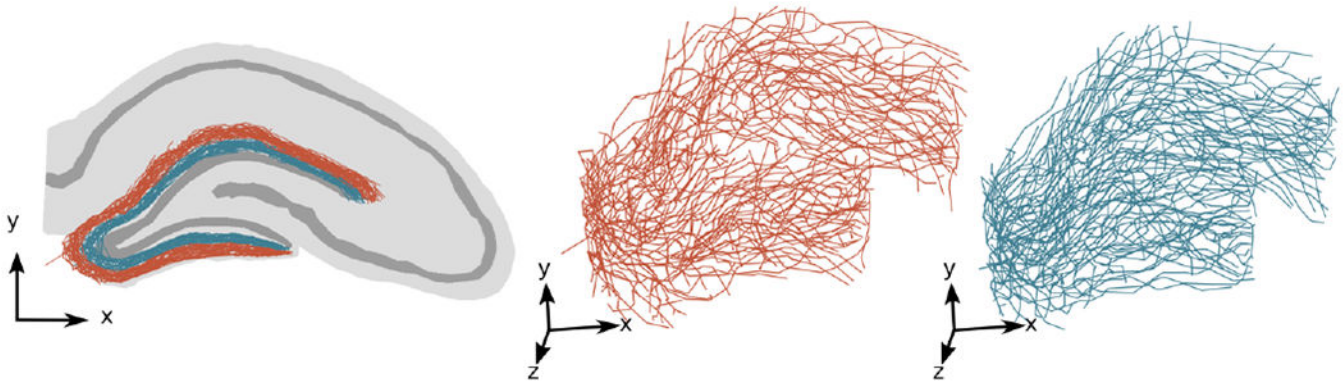

Figure 3.

Example graph models (red, LEC; teal, MEC) of entorhinal cortical axon terminal fields, generated by the proposed algorithm. These axons have features expected in *in situ* fibers, namely: *en passage* terminal topography, laminar architecture (i.e. MEC/LEC are spatially segregated within the dentate molecular layer), and fibers proceed to the ends of each supra/infrapyramidal blade of the dentate gyrus.

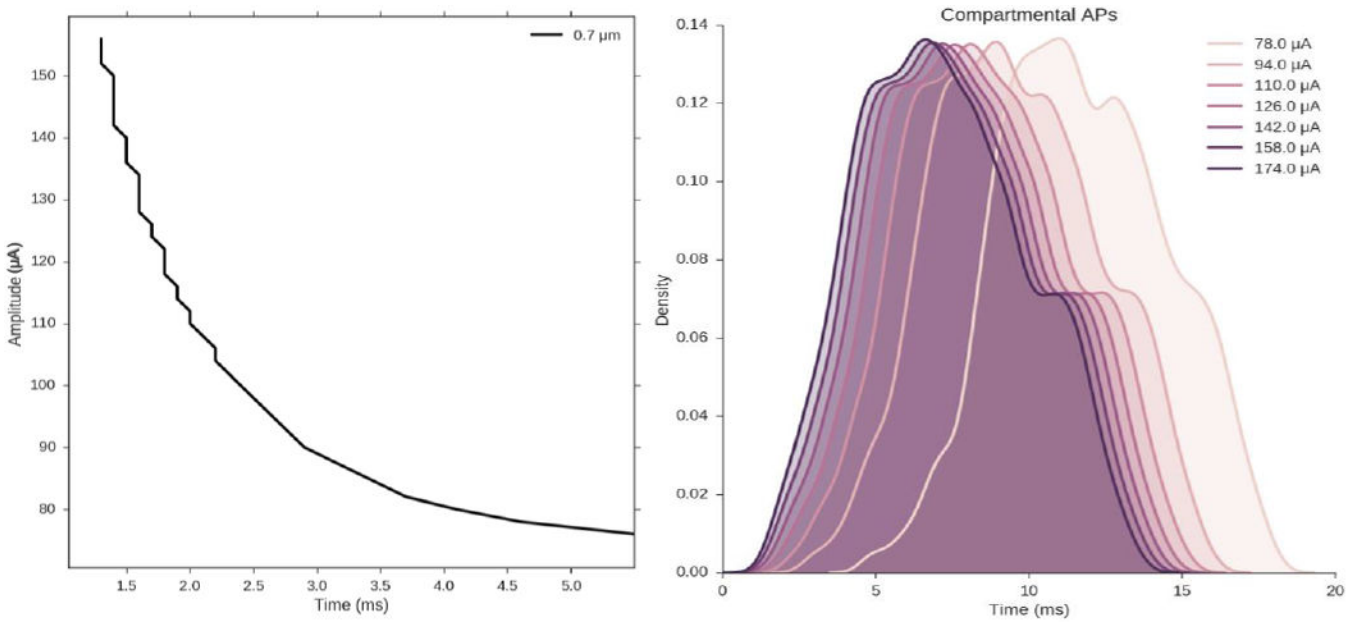

Figure 4.

(A) Strength-duration curve for 0.7 um diameter fibers at electrode-fiber distance of 250um and very long duration current-controlled pulses. Each data point represents the time to first action potential for a given pulse amplitude. (B) Kernel density estimates for compartmental action potential delays in arbor of 0.7um fiber diameter.